15A.2 A STUDY OF DIAGNOSTIC ESTIMATES OF SPATIAL ERROR CORRELATIONS FOR AMSU-A TYPE OBSERVATIONS

Rishabh Bhatt*[1], Massimo Bonavita[2], Niels Bormann[2], Sarah L Dance[1,4], Alison Fowler[1,4], Christopher Merchant[1,4], Jonathan Mittaz[1,5], Stewart Newman[3], and Joanne Waller[3]

[1]University of Reading, Reading, United Kingdom
[2]European Centre for Medium-Range Weather Forecasts, Reading, United Kingdom
[3]Met Office, Exeter, United Kingdom
[4]National Centre for Earth Observation, University of Reading, United Kingdom
[5]National Physical Laboratory, Teddington, United Kingdom

1. INTRODUCTION

Current numerical weather prediction (NWP) systems have long benefited from different satellite missions that provide information about a variety of model variables. However, despite the massive volume of available observations, many of these are discarded for NWP, in part due to problems with accounting for spatial observation error correlations (Dando et al. 2007). To avoid treatment of correlated errors, satellite radiances are generally thinned at operational centres prior to assimilation (Duncan et al. 2024). This comes with a significant reduction in the number of observations and information content in meteorologically interesting regions such as areas of deep convection or tropical cyclones (Fowler et al. 2018). To improve forecast skill for high impact weather events, it is essential that correlated observation errors are appropriately accounted for in data assimilation systems.

Our focus here is on the observations from AMSU-A. It is one of the most impactful satellite instruments due to its strength in numbers and tropospheric channels' sensitivity primarily to air temperature (Duncan et al. 2021, 2022). The current operational thinning distance used by ECMWF for AMSU-A observations is 125 km. The top image in Figure 1 shows the NOAA-18 AMSU-A observation density over North-western Europe on 01 Nov 2023 00UTC for the operational thinning distance. The bottom image shows a potential five-fold increase in the observation density for the same area if the thinning distance is reduced to 31 km. The sampling of AMSU-A is around 48 km at nadir and increases towards the swath edges, so a thinning of 31 km effectively includes all AMSU-A observations.

Increasing the resolution of the data without accounting for observation error correlations could have detrimental effect on forecast skill (Liu and Rabier 2003). To demonstrate the impact of reduced thinning, we present results from data assimilation experiments using different AMSU-A thinning lengths, based on the ECMWF IFS cycle 48r1 (ECMWF 2023). The experiments include operational thinning (N80: 125 km) of AMSU-A data as the control, alongside varying AMSU-A thinning distances of 177, 111, 89, 71, and 31 km. They use a 12-hour cycle 4D-Var, a full observing system and are run at IFS resolution Tco399 on an octahedral reduced Gaussian grid with approximately 28 km grid spacing (ECMWF 2019). Figure 2 shows the normalised change in standard deviation of observation minus background ($\mathbf{O}-\mathbf{B}$) for geopotential at 500 hPa across the southern hemisphere (left), the tropics (middle) and the northern hemisphere (right). Values above and below zero indicate a degradation and an improvement compared to operational thinning respectively. The vertical lines give the 95% confidence levels. It can be seen that there is a degradation in forecast skill when more observations are added (i.e. thinning is reduced) in the tropics and the northern hemisphere. This is indicative of the sub-optimal use of the observations due to unaccounted for error correlations. However, there is an improvement in the southern hemisphere, particularly for the 71 km (red) and 31 km (black) thinning experiments which is likely due to the lack of other observations in that region.

The purpose of our work here is to estimate the spatial observation error correlations for AMSU-A by using the well known Desroziers et al. (2005) method and to identify the sources of these correlations so that we can ultimately model and account for them in the data assimilation system. In section 3 we present results for the NOAA-18 AMSU-A observation channels that exhibit significant correlations and reveal how the apparent correlations change when the data is stratified based on land

*Corresponding author address: Rishabh Bhatt, Univ. of Reading, Dept. of Meteorology, Reading, Berkshire, RG6 6ET; e-mail: r.bhatt@reading.ac.uk.

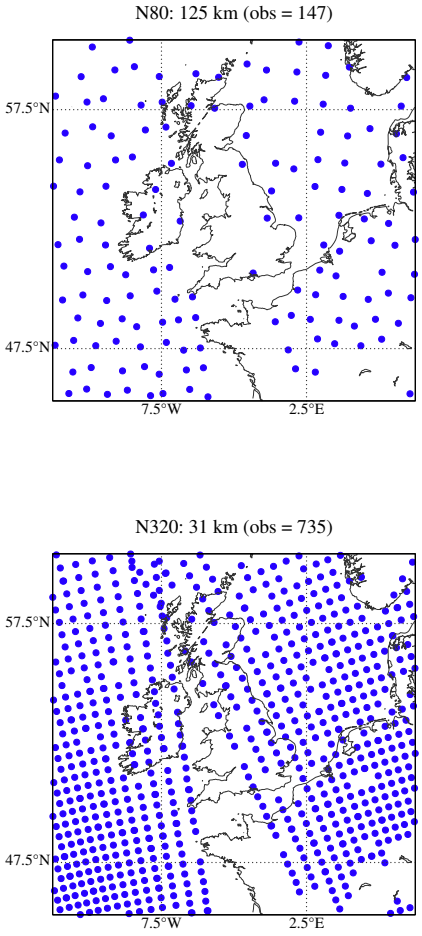


FIG. 1. AMSU-A observation thinning: used operationally at ECMWF (top) vs possible thinning if spatial error correlations are accounted for (bottom) The blue dots represent the areas where the observations are located.

and sea. Prior to that, we will provide a brief overview of the Desroziers et al. (2005) method and the AMSU-A all-sky observations in section 2.

2. METHODOLOGY

Data assimilation combines observations $\mathbf{y} \in \mathbb{R}^m$ with some previous forecast (background) $\mathbf{x}^b \in \mathbb{R}^n$ to provide an optimal initial state (analysis) $\mathbf{x}^a \in \mathbb{R}^n$. A typical 4D-Var cost function for a control initial state $\mathbf{x}_0$ is written as

$$J(\mathbf{x}_0) = \frac{1}{2}(\mathbf{x}^b - \mathbf{x}_0)^T \mathbf{B}^{-1}(\mathbf{x}^b - \mathbf{x}_0) + \frac{1}{2}\sum_{i=1}^{N}(H_i(\mathbf{x}_i) - \mathbf{y}_i)^T \mathbf{R}^{-1}(H_i(\mathbf{x}_i) - \mathbf{y}_i) \quad (1)$$

where $\mathbf{B}$ and $\mathbf{R}$ are the covariance matrices assigned for background and observation errors respectively. $H_i : \mathbb{R}^n \to \mathbb{R}^m$ is the observation operator that maps the model state onto the observation space. That is,

$$\mathbf{y}_i = H_i(\mathbf{x}^t) + \varepsilon_o. \quad (2)$$

where $\mathbf{x}^t$ is the true state. ε_o is the observation error which includes instrument error and the representative errors due to the observation operator, preprocessing or quality control, and unresolved scales in the model (Janjić et al. 2018).

Estimating observation error covariances

To estimate the observation error covariance matrix $\mathbf{R}$, we use the well-known Desroziers et al. (2005) method. The method relies on a key assumption that the observation and background errors are uncorrelated. It is based on the statistical expectation of the outer product of observation minus analysis ($\mathbf{d}_a^o$) and observation minus background ($\mathbf{d}_b^o$) residuals (in our case, we are using debiased residuals). In other words,

$$\mathbf{R} \approx \mathbb{E}[\mathbf{d}_a^o (\mathbf{d}_b^o)^T] \approx \frac{1}{N}\sum_{i=1}^{N}(\mathbf{d}_a^o|_i - \bar{\mathbf{d}}_a^o)(\mathbf{d}_b^o|_i - \bar{\mathbf{d}}_b^o)^T \quad (3)$$

where

$$\mathbf{d}_a^o = \mathbf{y} - H(\mathbf{x}^a), \quad (4)$$

$$\mathbf{d}_b^o = \mathbf{y} - H(\mathbf{x}^b) \quad (5)$$

and N is the total number of samples. For a given sample size, N, we can bin each $\mathbf{d}_a^o$ and $\mathbf{d}_b^o$ pair in different ways to describe correlations as a function of e.g. surface type, latitude, cloud fraction, scan angle etc. To calculate spatial observation error correlations, the data is binned as a function of the separation distance between the $\mathbf{d}_a^o$ and $\mathbf{d}_b^o$ pairs. Here we are going to apply this method on the all-sky AMSU-A observations.

All-sky AMSU-A

The Advanced Microwave Sounding Unit (AMSU-A) is a 15 channel microwave sounder whose primary task is to provide atmospheric temperature

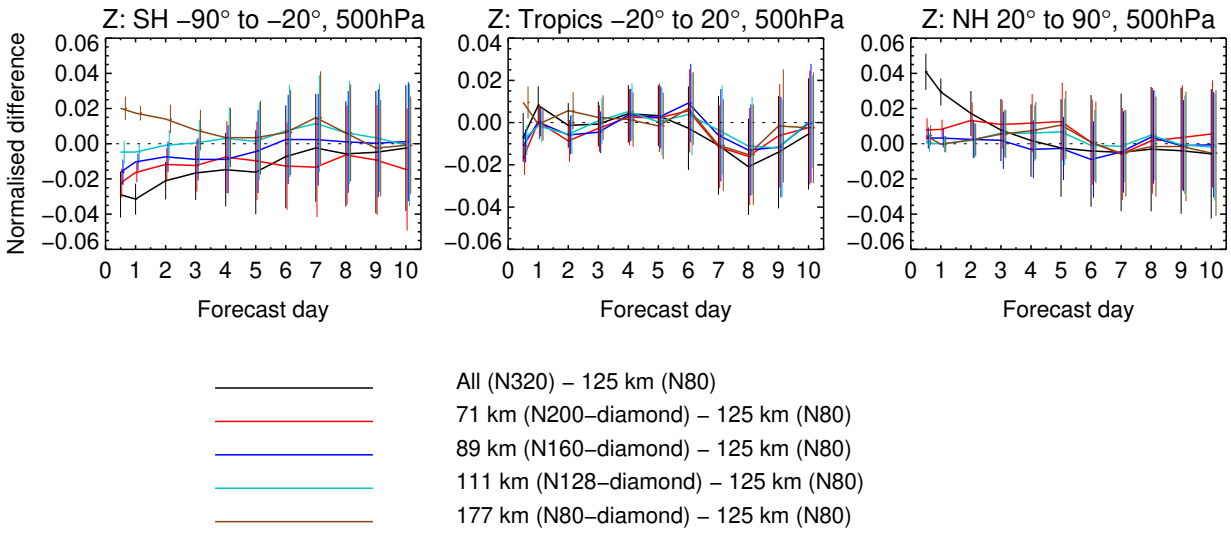


FIG. 2. Normalised change in standard deviation of $\mathbf{O}-\mathbf{B}$ for geopotential at 500hPa across the southern hemisphere (left), the tropics (middle), and the northern hemisphere (right). The reference (0% line) is the N80 control experiment while the 31 km (black), 71 km (red), 89 km (blue), 111 km (light blue), and 177 km (brown) are the different thinning experiments. Vertical error bars indicate the 95 % confidence range; verification is against the control.

profiling 50 GHz oxygen band. It provides data sampled at 48 km across track resolution at nadir. Table 1 shows the AMSU-A channels and their sensitivity in the atmosphere.

A key difference between AMSU-A all-sky and AMSU-A clear-sky assimilation is the way cloud affected radiances are treated. In clear-sky assimilation these radiances are simply discarded during quality control and the observation operator is based on clear-sky radiative transfer only. In contrast, in all-sky assimilation, data is used in clear, cloudy, and rainy scenes and model clouds are taken into account in the radiative transfer. A situation dependent error model is used where a higher error is provided on top of a baseline error in the presence of clouds (Duncan et al. 2022). From the table it can be seen that channels 4-9 are sensitive to troposphere where most of the clouds are present.

Channel	Frequency (GHz)	Peak sensitivity (hPa)
1	23.8	surface
2	31.4	surface
3	50.3	surface
4	52.8	$920-810$
5	53.596 ± 0.115	$650-530$
6	54.4	$390-320$
7	54.94	$260-200$
8	55.5	$170-135$
9	$57.29=f_0$	$85-70$
10	$f_0\pm0.217$	$50-40$
11	$f_0\pm0.3222\pm0.048$	$25-20$
12	$f_0\pm0.3222\pm0.022$	10
13	$f_0\pm0.3222\pm0.010$	5
14	$f_0\pm0.3222\pm0.0045$	3
15	89.0	surface

TABLE 1. Information on AMSU-A channels.

Data

Our estimates are computed using operational data from ECMWF's IFS cycle 48r1, run at model resolution Tco1279 (ECMWF 2019) which is around 9 km. The $\mathbf{O}-\mathbf{A}$ and $\mathbf{O}-\mathbf{B}$ residuals are stored as part of the process in MARS (Meteorological Archival and Retrieval System) and can be easily retrieved. AMSU-A all-sky observations are taken from NOAA-18 for the month of November 2023. The observations are thinned at 125 km and the correlations are plotted by taking samples binned at 25 km separation distances following Bormann and Bauer (2010). The estimates are calculated from a sample size N (for channel 5,6,7) of around 1 million observations. From the sample size, roughly

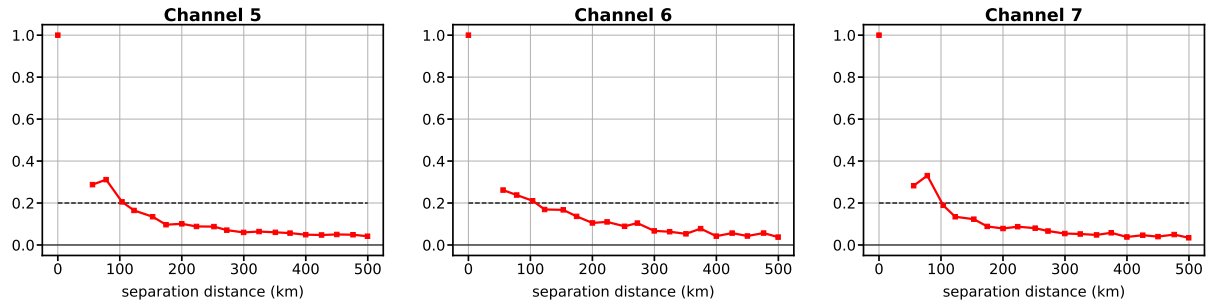


FIG. 3. Estimated spatial observation error correlations for AMSU-A channels 5,6,7 on NOAA-18. The correlations (red) are plotted as a function of separation distance between the samples with the squares being the distance bins. The black dashed line at 0.2 indicates the level after which the correlations become significant.

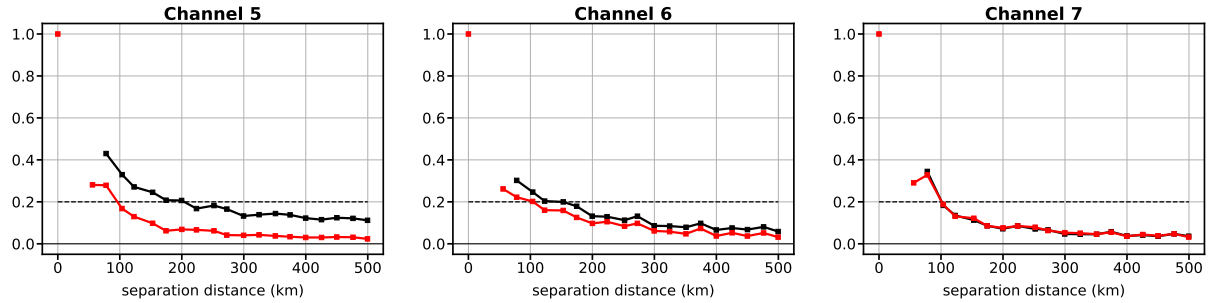


FIG. 4. A comparison of the estimated spatial observation error correlations for AMSU-A channels 5,6,7 on NOAA-18 as a function of separation distance when observations are over land (black) vs over sea (red). The black dashed line at 0.2 is again the threshold after which correlations become significant.

800,000 observations are over sea and 200,000 observations are over land. As a rule of thumb, correlations are assumed to be insignificant if they are less than 0.2 (Liu and Rabier 2003).

3. RESULTS

NOAA-18

The initial estimates show high spatial observation error correlations for lower peaking channels, in particular for channels 5,6, and 7. These are the channels which are more sensitive to the surface, and precipitation and where the situation dependent observation error modelling is applied. Figure 3 shows the correlation for these channels where we can see the correlation length scales (defined here as the distance where the correlation drops below 0.2) to be $\sim$ 100 km. Similar estimates are found for AMSU-A on NOAA-15, NOAA-19, MetOp-B and MetOp-C for the same channels which are not shown here. On the other hand, the higher peaking channels 8-14 have negligible error correlations (also not shown). We speculate that the higher correlation in the lower peaking channels is down to the error due to the misrepresentation of clouds in the radiative transfer model as these channels are more sensitive to the surface, and to clouds and precipitation.

Land vs sea

We show again the results for the same channels from NOAA-18 but when data is stratified based on whether observations are taken over land or over sea (see Figure 4). The correlation estimates differ for land and sea for channels 5 and 6 with the correlation being higher over land than over sea. For channel 5, the correlation length scale for land ($\sim$ 175 km) is considerably larger compared to the correlation length scale for sea ($\sim$ 100 km). Our results are similar to the study conducted by Bormann and Bauer (2010) for the clear-sky AMSU-A data.

Higher correlation over land suggests misspecification of surface emissivity and surface skin temperature in the radiative transfer model but further evidence is required to establish the definitive source of error correlations.

4. CONCLUSION

In this work we present initial results examining spatial observation error correlation estimates for AMSU-A during November 2023 using the Desroziers et al. (2005) method. The correlations were found to be higher for the surface sensitive channels (5,6, and 7) and negligible for the higher peaking channels. When stratified based on surface type, the correlations for observations over the land were much higher compared to those over sea for channels 5 and 6. Our next step is to pinpoint the sources of uncertainty. It is also important to note that these estimates are not perfect as they depend on the assumed statistics for the background and observations (Waller et al. 2016; Hu and Dance 2024). A thorough metrological study (Mittaz et al. 2019) can provide valuable insights into these sources such as instrument calibration, scanning geometry, and model biases. Moreover, metrology will help establish a lower bound and provide confidence in our estimates.

Acknowledgements

This work was supported by University of Reading's Advancing the Frontiers of Earth Prediction System (AFESP) research programme.

REFERENCES

Bormann, N., and P. Bauer, 2010: Estimates of spatial and interchannel observation-error characteristics for current sounder radiances for numerical weather prediction. i: Methods and application to atovs data. *Quarterly Journal of the Royal Meteorological Society*, **136 (649)**, 1036–1050.

Dando, M., A. Thorpe, and J. Eyre, 2007: The optimal density of atmospheric sounder observations in the met office nwp system. *Quarterly Journal of the Royal Meteorological Society: A journal of the atmospheric sciences, applied meteorology and physical oceanography*, **133 (629)**, 1933–1943.

Desroziers, G., L. Berre, B. Chapnik, and P. Poli, 2005: Diagnosis of observation, background and analysis-error statistics in observation space. *Quarterly Journal of the Royal Meteorological Society: A journal of the atmospheric sciences, applied meteorology and physical oceanography*, **131 (613)**, 3385–3396.

Duncan, D. I., N. Bormann, A. J. Geer, and P. Weston, 2022: Assimilation of amsu-a in all-sky conditions. *Monthly Weather Review*, **150 (5)**, 1023–1041.

Duncan, D. I., N. Bormann, A. J. Geer, and P. Weston, 2024: Superobbing and thinning scales for all-sky humidity sounder assimilation. *Monthly Weather Review*.

Duncan, D. I., N. Bormann, and E. V. Hólm, 2021: On the addition of microwave sounders and numerical weather prediction skill. *Quarterly Journal of the Royal Meteorological Society*, **147 (740)**, 3703–3718.

ECMWF, 2019: Introducing the octahedral reduced gaussian grid. URL http://confluence.ecmwf.int/display/FCST/Introducing+the+octahedral+reduced+Gaussian+grid.

ECMWF, 2023: Ifs documentation cy48r1, part ii: data assimilation. URL http://www.ecmwf.int/en/elibrary/81368-ifs-documentation-cy48r1-part-ii-data-assimilation.

Fowler, A., S. Dance, and J. Waller, 2018: On the interaction of observation and prior error correlations in data assimilation. *Quarterly Journal of the Royal Meteorological Society*, **144 (710)**, 48–62.

Hu, G., and S. L. Dance, 2024: Sampling and misspecification errors in the estimation of observation-error covariance matrices using observation-minus-background and observation-minus-analysis statistics. *Quarterly Journal of the Royal Meteorological Society*.

Janjić, T., and Coauthors, 2018: On the representation error in data assimilation. *Quarterly Journal of the Royal Meteorological Society*, **144 (713)**, 1257–1278.

Liu, Z.-Q., and F. Rabier, 2003: The potential of high-density observations for numerical weather prediction: A study with simulated observations. *Quarterly Journal of the Royal Meteorological Society: A journal of the atmospheric sciences, applied meteorology and physical oceanography*, **129 (594)**, 3013–3035.

Mittaz, J., C. J. Merchant, and E. R. Woolliams, 2019: Applying principles of metrology to histori-

cal earth observations from satellites. *Metrologia*, **56 (3)**, 032 002.

Waller, J. A., S. L. Dance, and N. K. Nichols, 2016: Theoretical insight into diagnosing observation error correlations using observation-minus-background and observation-minus-analysis statistics. *Quarterly Journal of the Royal Meteorological Society*, **142 (694)**, 418–431.